Preconditioning Prefrontal Connectivity Using Transcranial Direct Current Stimulation and Transcranial Magnetic Stimulation

Isabel Alkhasli (isabel.alkhasli@b-tu.de)
Uniklinik RWTH Aachen: Universitatsklinikum Aachen https://orcid.org/0000-0001-6264-6307
Felix M. Mottaghy
Universitatsklinikum Aachen
Ferdinand Binkofski
Uniklinik RWTH Aachen: Universitatsklinikum Aachen
Katrin Sakreida
Uniklinik RWTH Aachen: Universitatsklinikum Aachen

Research Article

Keywords: Functional Connectivity, Preconditioning, DLPFC, TMS, tDCS, Resting State

Posted Date: January 5th, 2022

DOI: https://doi.org/10.21203/rs.3.rs-1177712/v1

Version of Record: A version of this preprint was published at Frontiers in Human Neuroscience on August 11th, 2022. See the published version at https://doi.org/10.3389/fnhum.2022.929917.

Abstract

Transcranial direct current stimulation (tDCS) and transcranial magnetic stimulation (TMS) have been shown to modulate functional connectivity. Their specific effects seem to be dependent on the pre-existing neuronal state. We aimed to precondition frontal networks using tDCS and subsequently stimulate the left dorsolateral prefrontal cortex (lDLPFC) using TMS. Thirty healthy participants underwent either excitatory, inhibitory or sham tDCS for 10 min, as well as an excitatory intermittent theta burst (iTBS) protocol (600 pulses in 190 s, 20 x 2 s trains), applied over the lDLPFC at 90% of the individual resting motor threshold. Functional connectivity was measured in three task-free, 10-min-long baseline resting state fMRI sessions, immediately before and after tDCS, as well as after iTBS. Connectivity analyses between stimulation site and all other brain voxels, contrasting the interaction effect between the experimental tDCS groups (excitatory vs inhibitory) and the repeated measure (post tDCS vs. post TMS), revealed significantly affected voxels bilaterally in the anterior cingulate and paracingulate gyri, the caudate nuclei, the insula and operculum cortices, as well as the Heschl's gyrus. ROI-to-ROI analyses additionally showed temporo-parietal-striatal and temporo-parietal-fronto-cingulate differences between the anodal and cathodal group post tDCS, as well as striatal-temporo-parietal anodal-cathodal differences and frontostriatal cathodal-sham group differences post TMS. Excitatory iTBS to a tDCS-inhibited lDLPFC yielded stronger functional connectivity to various areas, as compared to excitatory iTBS to a tDCS-enhanced prefrontal cortex. Results demonstrate complex, whole-brain stimulation effects, most-likely facilitated by cortical homeostatic control mechanisms, as well as the feasibility of using tDCS to modulate TMS effects.

Introduction

The notion of homeostatic plasticity in the neuronal system has been studied in animal research using electrical microstimulation for about 30 years (Bear and Malenka 1994; Hess and Donoghue 1996; Iriki et al. 1989). The neuronal system strives to keep cortical excitability in a physiologically optimal level by adjusting to internal and external inputs in the form of short- as well as long-term potentiation (STP/LTP) or depression (STD/LTD). Whereas STP/STD works through the temporal change of presynaptic processes that causes a change in the firing threshold of the neuron and only lasts for about 15 min, LTP/LTD is the persistent increase in synaptic strength between neurons. This mechanism of plasticity of the brain also effects communication between larger cell clusters and thus plays an important role in motor learning and memory (Asanuma and Keller 1991; Rioult-Pedotti et al. 2000).

There have been numerous studies indicating the possibility to manipulate homeostatic plasticity using non-invasive brain stimulation methods. Siebner, Lang and colleagues (Lang et al. 2004; Siebner et al. 2004) reported the first demonstration of the mechanism of homeostatic plasticity in the human primary motor cortex. They showed that the effects of transcranial magnetic stimulation (TMS) can be amplified by a preconditioning transcranial direct current stimulation (tDCS). Interestingly they documented a paradoxical effect: Both high frequency TMS, which is known to have a facilitating effect, but also a low frequency TMS protocol, that is typically inhibitory, were able to amplify cortical excitability when applied

to the motor hand area that was preconditioned with cathodal (inhibitory) tDCS or hamper cortical excitability when applied after anodal (excitatory) tDCS. The effect of the inhibitory or excitatory tDCS on corticospinal excitability, measured as the amplitude of motor-evoked potentials (MEPs) induced by a single TMS pulse applied to the cortical hand area and derived from one hand muscle, was thus inversed in polarity by any of the tested TMS protocols. This phenomenon has since been replicated repeatedly in the motor system and its physiological mechanisms are well understood (Cosentino et al. 2012; Fregni and Pascual-Leone 2007; Fricke et al. 2011). For example, Grüner et al. (2010), where able to decrease involuntary movements of the fingers and hands in patients with Parkinson's disease using inhibitory tDCS and TMS of the primary motor cortex. Carvalho et al. (2015) were able to enhance working memory performance using tDCS preconditioning with different polarities and thus demonstrated that the polarity effect of tDCS is dependent on the precondition of the neuronal population and that stimulation effects are functional significant in the memory domain.

Repetitive TMS (rTMS) has been shown to be able to increase as well as decrease synaptic excitability in a focal cortical area (Sparing and Mottaghy 2008). Even though rTMS does not directly influence subcortical areas, numerous studies showed rTMS induced changes in cortical-subcortical functional connectivity (e.g. Bestmann et al. 2004; Fox et al. 2012; Paus et al. 2001; Shafi et al. 2012; Siebner et al. 1998) . TDCS on the other hand, works through the placement of two electrodes on the scalp inducing a non-focal current in the brain. Rather than triggering acute action potential in the neurons, as seen as a result of TMS, tDCS causes subtle negative (anodal) or positive (cathodal) shifts in the membrane polarity. The notion of functional connectivity as a simple measure of synchrony between BOLD-time courses of single voxels or region of interests. It's commonly expressed as a Fisher-z transformed correlation value and has been used as a measure of communication between neuronal clusters, as it is argued that high synchrony of neuronal firing indicates a functional connection even in the absence of direct anatomical links.

The dorsolateral prefrontal cortex (DLPFC) has been shown to play a central role in the cognitive control of behaviour and other executive functions, such as attention, motor planning, procedural memory, as well as reward and emotion. Its various cortical and subcortical interconnections make it an ideal target for non-invasive brain stimulation studies (Dedoncker et al. 2016; Guse et al. 2010). It is functionally interconnected with the orbitofrontal cortex, large parts of the neocortex, the parietal cortex, the cingulate cortex, and the subcortical basal ganglia, thalamus and hippocampus (Alexander et al. 1986; Petrides and Pandya 1999; Tekin and Cummings 2002; Tik et al. 2017). Animal studies demonstrated that the frontal cortex controls the release of dopamine in the striatum (Kanno et al. 2004; Karreman and Moghaddam 1996; Keck et al. 2002; Murase et al. 1993). Disruption in the balance of the neurotransmitter glutamate and dopamine in the striatum has been observed to cause aggressive and impulsive behaviour, and has been linked to neurodegenerative diseases, such as Parkinson's disease and dementia syndrome, as well as to psychiatric diseases such as schizophrenia (Carlsson and Carlsson 1990; Strafella et al. 2005). In a landmark study using TMS and positron emission tomography (PET), Strafella et al. showed that in human subjects dopamine release was increased following the stimulation of the DLPFC (Strafella et al. 2001) as well as the left primary motor cortex (Strafella et al. 2003). This

connection opens the possibility for potential therapeutic use of preconditioning and modulating the DLPFC via non-invasive brain stimulation.

This study aimed to answer the question whether the concept of preconditioning can be transferred to the human prefrontal cortex and whether an effect can be observed in terms of functional connectivity pattern between the stimulation site and its connected areas. Some previous neuroanatomical and electrophysiological studies have aimed at the mechanism of the modulation of the prefrontal function and found it to be much more complex when compared to the primary motor cortex (Alkhasli et al. 2019; Kähkönen et al. 2005; Keeser et al. 2011; Nahas et al. 2001; Tremblay et al. 2014). Our goal was to utilize homeostatic plasticity in the prefrontal cortex to explore whole brain connectivity and more specifically, fronto-cortical and frontostriatal connectivity in task-free resting state functional magnetic resonance imaging (rsfMRI). Functional connectivity can be measured using Pearson correlation of the BOLD timelines of two regions of interest (ROIs) and expresses to what extent their communication is coupled. Here, we aimed to precondition the excitatory rTMS stimulation of lDLPFC by using either excitatory, inhibitory or sham tDCS. At baseline, after the tDCS as well as after a subsequent excitatory 190 s long intermittent theta burst stimulation (iTBS) protocol we compared frontostriatal functional connectivity between the three differently preconditioned groups of participants using rsfMRI. We aimed at the question whether homeostatic plasticity can be used to precondition the network and enhance or hinder functional connectivity of the frontostriatal network using tDCS and TMS. In this respect we analysed the differential effect of anodal, cathodal, and sham tDCS on functional connectivity of the brain. The striatum was chosen as an additional ROI because of its significant functional connection with the DLPFC and its clinical significance as part of dopaminergic nigrostriatal pathway.

Materials And Methods

2.1 Participants

Thirty neurologically and mentally healthy, right handed (validated by the Edinburgh Handedness Inventory (Oldfield 1971) participants were recruited (mean age = 25.5, SD = 5.14; 15 male). Participants were pre-screened for TMS, tDCS and magnetic resonance imaging (MRI) exclusion criteria.

2.2 Experimental procedure

An overview of the experimental procedure and the durations is shown in Figure 1. In all participants, a high-resolution anatomical MRI scan (see TMS and MRI sections below) was measured and the individual resting motor threshold (rMT) was determined using a standardised protocol (Rossi et al. 2009; Rossini et al. 2015). Afterwards the first of three identical rsfMRI measurement was collected for each participant, lasting about 10 min. During the scan participants were shown a small black fixation spot in the middle of a grey background. They were instructed to fixate the dot at all times, to relax, don't fall asleep, lie as still as possible, and to try not to think of anything in particular. For the following

application of brain stimulation by use of tDCS and TMS the participant was brought outside the scanner room but was lying supine on the mobile scanner bed for the entire experiment. After registration with individual anatomical MRI data (see MRI section below for scanning parameters) tDCS was applied over the lDLPFC using neuronavigation (see section ‘Transcranial direct current stimulation’ for more details) for 10 min with either anodal (10 participants), cathodal (10 participants) polarity, or sham tDCS with either anodal or cathodal polarity (10 participants). Blinding for the tDCS protocol was assessed after all experimental procedures by asking the participants whether they knew they had received real or control stimulation and whether they had experienced any unpleasant sensations. After tDCS, participants underwent the second rsfMRI measurement, before they received iTBS lasting 190 secs, applied over the lDLPFC using neuronavigiation (see section ‘Transcranial magnetic stimulation’ for more details) at 90% of individual rMT. After a 7-min-break the participants were rolled into the scanner again, lying in an unchanged position on the scanner bed and the last 10-min-post TMS rsfMRI measurement was conducted. This 7-min interval was kept constant between all participants and was implemented to allow for arousal and discomfort ratings and MRI preparations. Immediately after each stimulation, arousal was assessed using a 9-level self-assessment manikin (SAM) scale with level 1 corresponds to 'very calm and relaxed” and level 9 corresponds to ‘very excited, stimulated, furious, excited, aroused’ (Bradley and Lang 1994). After TMS, an additional 5-level Likert scale was used to measure discomfort during iTBS stimulation (1 = none, 5 = strong). To test whether arousal or discomfort was significantly different between the tDCS groups or measurement points, non-parametric tests were conducted.

2.3 Transcranial direct current stimulation

TDCS was administered either as anodal (1mA), cathodal (- 1mA) or sham (0mA, either anodal or cathodal electrode placement) stimulation using a MRI-compatible stimulator (neuroConn GmbH, Ilmenau, Germany). The fade-in/out period was 10 s. The placement of the active electrode sized 5 by 7 cm was thereby determined by transforming the individual anatomical images into the MNI system using the neuronavigation system (LOCALITE Biomedical Visualization Systems GmbH, Sankt Augustin, Germany) and marking the MNI coordinates (x, y, z) = -50, 30, 36 with the neuronavigation pointer as stimulation target. These coordinates were suggested by Rusjan et al. (2010) for an optimal location of the lDLPFC by neuronavigation as compared to conventional distance-based localization methods. The tDCS reference electrode sized 10 by 10 cm was placed contralateral and supraorbital. The stimulation was applied for 10 min. As during rsfMRI, participants were instructed to relax, don’t fall asleep, lie as still as possible, and to try not to think of anything in particular, but they could close their eyes.

2.4 Transcranial magnetic stimulation

Both, single pulse TMS for determination of the individual rMT and the experimental iTBS was applied using a figure-of-eight coil (C-B60) connected to a MagPro X100 stimulator (MagVenture, Farum, Denmark) guided by neuronavigation. In preparation of rMT determination, the presumed hand area was

identified visually through anatomical landmarks in the left motor cortex. Participants were placed in a comfortable chair or lying down on the MRI scanner bed outside the scanner room for registration with their individual anatomical MRI data. Three pre-gelled disposable surface electrodes were fitted to the participant's right hand (first dorsal interosseous muscle, index finger, inner wrist) to derive MEPs which were monitored on the MEP Monitor (MagVenture, Farum, Denmark) connected to the MagPro X100 stimulator. Biphasic single pulses were applied over the presumed hand area starting at 30% of stimulator output but was increased until clear MEPs and hand muscle contraction could be observed. Intensity was then reduced stepwise to find the lowest intensity that induces supra-threshold (> 50 μV) MEPs above chance, i.e., we used the common rule that the rMT corresponds to the minimum stimulation intensity at which MEPs of at least 50 μV are elicited in at least 5 of 10 consecutive trials (50%) in the resting target muscle (Rossini et al. 2015).

The experimental excitatory iTBS (Huang et al. 2005) protocol consisted of 600 pulses spaced-out over 3 min and 20 seconds. It was comprised of 20 trains and 10 theta-bursts. Between each of the 2 sec-long trains (50 Hz) there was an 8 sec long pause. The lDLPFC stimulation site was determined the same as the tDCS target. Actual individual stimulation sites were recorded during the TMS procedure and used as subject specific seed regions. Participants received a stimulation at an intensity of 90% of their individual rMT. The mean rMT was 45.63 % (*SD* = 6.82) of the maximum stimulator output and the mean stimulation applied was 41.01 % (*SD* = 5.68) of the maximum stimulator output. The stimulation threshold of 90% of the individual resting motor threshold was chosen based on related experiments by our group that found a strong frontostriatal modulation effect at that threshold (Alkhasli et al. 2019).

Simultaneously with each TMS pulse, stimulation markers, including the information of exact position of the coil hotspot and its perpendicular projection onto the brain surface, were recorded by the neuro-navigation system. For each participant, we exported one of the first stimulation marker as volume of interest into the NIfTI file format for further image analyses.

2.5 Magnetic resonance imaging

MRI scans were measured on a Magnetom Prisma 3.0 T whole-body scanner (Siemens Medical Solutions, Erlangen, Germany). Anatomical data was acquired using a three-dimensional magnetization-prepared, rapid acquisition gradient-echo sequence (MP-RAGE) with the following parameter: 300 repetitions, TR = 2300 ms, TE = 2.98 ms, 9º flip angle, FOV = 256 mm, 176 sagittal slices, slice thickness = 1 mm and in-plane resolution = 1 × 1 × 1mm.

RsfMRI data were measured with a gradient echo planar imaging (EPI) sequence with the following parameters: TR = 2000 ms, TE = 28 ms, 77º flip angle, FOV = 192 mm, 34 axial slices (interleaved acquisition), 3 mm slice thickness, echo planar imaging volumes and in-plane resolution = 3 × 3 × 3mm. Both sequences lasted about 10 min.

2.6 Pre-processing of resting state

MRI-data was analysed using the Statistical Parametric Mapping software SPM12 (Welcome Department of Cognitive Neurosciences, London, UK) and CONN Functional Connectivity version (18.b, Whitfield-Gabrieli and Nieto-Castanon 2012) toolboxes running under Matlab R2012b (MathWorks Inc., Natick, MA, USA). Pre-processing of the rsfMRI data included: removal of first 5 volumes to discard saturation effects, slice time correction, realignment, segmentation, nuisance covariates regression with white matter and cerebrospinal fluid as regressors, head motion correction, head motion scrubbing as regressor, band pass filtering of the frequencies 0.01-0.08 Hz and linear detrending. The root-mean-square of the head motion translation parameters [displacement = square root ($x^2 + y^2 + z^2$)] across all participants and sessions was 0.13 mm (*Max* = 0.25 mm, *SD* = 0.05 mm), with a mean subject-wise maximum of 0.97 mm (*Max* = 3.07 mm, *SD* = 0.83 mm).

2.7 Functional connectivity

To explore the whole brain stimulation effect, seed-to-voxel correlations were calculated. For each subject the activity of the individual stimulation site (lDLPFC, a sphere with a diameter of 1cm) was extracted as an unweighted mean BOLD signal change time series. Three-dimensional stimulation seed masks where obtained from each participant's individual T1-anatomy and then co-registered with the corresponding functional data set. Functional connectivity was then calculated as a Fisher-Z-transformed correlation coefficient, between the stimulation site (lDLPFC, seed) signal and all individual voxel signals, separately. All correlation values are Fisher-Z-transformed. Alpha values inflation caused by multiple comparison was corrected on a cluster-size level.

To explore connectivity patterns specifically between the stimulation site and specific ROIs, ROI-to-ROI-analyses were calculated. Functional connectivity was additionally calculated using a three clusters extracted from the seed-to-voxel analysis, as well as a bilateral striatum masks (Harvard-Oxford atlas, consisting of caudate, putamen and nucleus accumbens). Striatal signal time series were thus extracted from MNI normalized functional data. In total there were four different seed masks: lDLPFC (stimulation site), three extracted clusters and the striatum.

Calculating a 3 × 3 mixed effect analysis of variance (ANOVA) of the functional connectivity between the stimulation site seed and each of the additional four ROIs (three clusters and striatum) resulted in four separate ANOVAs. For each ANOVA the within-subjects effect was the repeated measure (baseline vs. post-tDCS vs. post-TMS) and the between-subjects effect was the tDCS group (anodal vs. cathodal vs. sham tDCS).

Results

3.1 Whole brain stimulation effect: Seed-to-voxel-analysis

To identify clusters significantly affected by the two experimental stimulations (post tDCS and post TMS) an exploratory seed-to-voxel analysis was conducted. Contrasting only the interaction effect between the two factors 'preconditioning' (anodal tDCS vs. cathodal tDCS) and 'time point of post-stimulation measurement' (post-tDCS vs post-TMS) did yield three significant clusters [α = 5 % uncorrected voxel threshold and false discovery rate (FDR, Benjamini and Hochberg 1995)-corrected cluster-size, *df* = 18]. A visualization and summary of anatomical and statistical properties of the significant clusters can be found in Table 1 and Figure 2. There was a large bilateral cluster of 1638 voxels that covers mostly the cingulate and paracingulate gyrus, the frontal pole and small portions of the caudate in the subcortical basal ganglia. The two other smaller clusters covered large parts of insula and operculum and the Heschl's gyrus in both hemispheres.

3.2 Specific connectivity analysis: Region of interest (ROI) analysis

To visualize and further analyse network effects of the experiment, especially the involvement of the striatum, ROI-to-ROI analysis was conducted using the following five ROIs: lDLPFC (stimulation site), fronto-cingulate cluster (x, y, z = 4, 30, 14), left temporo-parietal cluster (x, y, z = -44, -26, 14 (), right temporo-parietal cluster (x, y, z = 42, -16, 8) and striatum. Mean ROI-to-ROI functional connectivity was extracted using CONN and visualised in Figure 2a. A summary of all ROI-to-ROI analysis results can be found in table 2. First, to test whether there was a significant effect of the whole experimental design on the functional connectivity between the five ROIs, a FDR-corrected, 3 × 3 ANOVAs for all ROI connections was conducted [n = 30, F(4,52), connection threshold: p < 0.05, FDR-corrected]. There was no significant effect. Nevertheless, as it can be seen in Figure 2b, all four ROI-pairs followed a similar pattern in terms of their functional connectivity patterns. The anodal (solid line) and cathodal (dashed line) groups showed an opposing trend, where the anodal group exhibited heightened connectivity post tDCS and lowered connectivity post TMS, whereas the cathodal group showed decreased connectivity after the tDCS and increased connectivity after the TMS. A one-way ANOVA testing of the sham group measurements of the three time points did not show a significant change in activity throughout the experiment for any of the 10 connections.

To compare functional network connectivity between the treatment groups at each of the post stimulation time points, multivariate post-hoc t-tests were calculated and the total alpha error was kept at 5% using a FDR approach. Results are summarized in Table 2 and Figure 2 b and c. Post tDCS, functional connectivity differed between the anodal and the cathodal group, as well as between the cathodal and the sham group. The anodal and the sham group did not show differential functional connectivity. The cathodal vs. anodal post tDCS contrast revealed two significant clusters comprised of lDLPFC to left and right temporo-parietal as well as striatal-right temporo-parietal and fronto-cingulate–left temporo-parietal cluster (connection cluster 1) and a lDLPFC to fronto-cingulate connection (connection cluster 2). The anodal vs. sham post tDCS contrast did show differences in terms of lDLPFC to fronto-cingulate connectivity. Post TMS, the anodal vs. cathodal contrast revealed two clusters comprised of a significant

lDLPFC-to-fronto-cingulate link (connection cluster 1) and two lDLPFC to left and right temporo-parietal connections, as well as a striatal-left temporo-parietal link (connection cluster 2). The post TMS cathodal vs. sham comparison showed lDLPFC connections to the fronto-cingulate and the striatum, respectively (connection cluster 1) and a fronto-striatal and a left and right temporo-parietal connection difference (connection cluster 2).

To summarize, in both post stimulation rsfMRI sessions, functional network connectivity differed significantly between the anodal and the cathodal group. Post tDCS, the cathodal and the sham group did not differ, and post TMS, the anodal and the sham group did not differ in terms of functional connectivity. In table 2, significant connections that were not already revealed in the seed-to-voxel analysis are marked with an underscore. That is, post tDCS, the anodal-cathodal differences involved the striatal-right temporo-parietal and fronto cingulate-left temporo-parietal connection, whereas post TMS, anodal-cathodal-differences involved the striatal-left temporo-parietal connection. Left-right-temporo-parietal and fronto-striatal connectivity was only different between the cathodal and sham group post TMS. Figure 2c shows that those connections additionally found in the ROI-to-ROI-analysis did not show the hypothesised pattern as clearly compared to the ROIs linked directly to the stimulation site in our analysis (compare Figure 2b).

3.3 Self-assessment manikin scale (SAMS) and blinding

Discomfort after TMS did not differ significantly between the tDCS groups (modal value = 4; Chi square = 4.37, p = .11, df = 2; Kruskal-Wallis test). There was no significant difference in the SAM arousal ratings between the tDCS groups at any point of the experiment (Chi square$_{Baseline}$ = 2.37, $p_{Baseline}$ = .31, Chi square$_{preTMS}$ = .11, p_{preTMS} = .95, Chi square$_{postTMS}$ = 1.51, $p_{postTMS}$ = ..47, df = 2, Kruskal-Wallis tests). 19 participants (63.33%) were not able to accurately tell whether they received experimental or sham tDCS.

Discussion

In this study we explored the possibility of preconditioning the prefrontal cortex. This was done by first administering excitatory, inhibitory, or sham tDCS and then facilitatory high-frequency rTMS (iTBS) to the lDLPFC. The tDCS was thus meant to prepare the network and possibly modulate the effects of TMS on the network. A whole brain analysis, testing for an interaction effect of the tDCS experimental group (anodal vs. cathodal) and the TMS effect (pre vs. post TMS) revealed three highly body-axial symmetric clusters of significant size. One cluster contained mainly voxels in the bilateral anterior cingulate and paracingulate gyri, as well as small portions of the bilateral caudate. The two other clusters covered mainly the insular cortices and operculum, as well as Heschl's gyri, bilaterally. Because of their bilateral location, as well as their anatomical and functional characteristics, it seems plausible that functional connectivity to the lDLPFC was indeed modulated by the experimental stimulation procedure. All clusters that were directly linked to the stimulation site in our results, showed the same activation pattern that was consistent with the notion of preconditioning. That is, the three groups started with a similar functional

connectivity to the stimulation site. Anodal tDCS then increased functional connectivity, while cathodal tDCS decreased functional connectivity of the stimulation site and the corresponding clusters. After TMS, this pattern got inversed, as the anodal group showed the lowest functional connectivity and the cathodal group ended up displaying the highest values. The sham group did not show a substantial change of functional connectivity throughout the experiment. These finding are consistent with the notion of homeostatic plasticity. That is, TMS applied to a system that was preconditioned shortly before by increasing or decreasing the membrane potential, did have a very different effect on functional connectivity. Our results thus show, for the first time, that the principles of homeostatic plasticity and preconditioning, that have previously been demonstrated in the motor cortex (Cosentino et al. 2012; Lang et al. 2004; Siebner et al. 2004), can be transferred to the prefrontal domain, and possibly extended to the anterior cingulate and paracingulate cortex, as well as the insular, operculum and Heschl's gyri.

The hypothesised and observed interaction effect between experimental groups and stimulation time points was strongest in the prefrontal-fronto-cingulate connection, but also significant in the bilateral frontal-temporo-parietal connections. A similar pattern, even if only significant at the post TMS measures was found in prefrontal-striatal connectivity. These areas are commonly linked to motivation and emotion (cingulate cortex, striatum), somatosensory and auditory function (paracingulate, insular, operculum and Heschl's gyrus) but also pain perception and evaluation (Eickhoff et al. 2006; Sawamoto et al. 2000; Wunderlich et al. 2011).

Emotions such as stress and anxiety have consistently been associated with an increase in frontostriatal connectivity (Arnsten 2009) and psychological states are likely to have a strong influence on the effectiveness of neuro-stimulation and vice versa (Carnevali et al. 2020). The mere physiological perception of pain or other stimulation related sensations can be ruled out as a cofounder to the post TMS results, since all three groups received the same treatment. We did not see a difference in arousal or pain ratings in our different tDCS groups and most participants were not able to accurately guess which tDCS stimulation they received. The observed data is thus likely to be affected by the stimulation protocol and should be functionally meaningful.

Stimulating the frontostriatal network as part of the clinically very significant dopaminergic pathway is a common goal in depression and Parkinson's treatment (e.g. Baggio et al. 2015; Bouyer et al. 1984; Carriere et al. 2015; Furman et al. 2011; Heller et al. 2013; Kang et al. 2016; Shine et al. 2013; Xu et al. 2016). Disordered fronto-cingulate connectivity has also been linked attention and mood disorders like depression (Pizzagalli 2011; Schlösser et al. 2008). Cho and Strafella (2009) did, for example, find an increase in dopamine release in the ipsilateral anterior cingulate and the orbitofrontal cortex following rTMS to the lDLPFC and frontostriatal.

Subjecting the data to ROI-to-ROI-analyses, to specifically answer the question whether frontostriatal communication can be modulated, did not yield a significant group effect for the whole design. However, we did find a pattern of frontostriatal functional connectivity in the whole-design-analysis, corresponding to the idea of a preconditioning effect. That is, functional connectivity between the lDLPFC and the

striatum was highest in the anodal tDCS group directly after the tDCS, as compared to the results of other groups at that measurement. The planned post-hoc comparisons of frontostriatal connectivity was significantly different between the anodal and sham group post TMS. This pattern corresponds to results found by other groups that found a facilitating effect of cathodal preconditioning and an inhibiting effect of anodal preconditioning on motor evoked potentials (Cosentino et al. 2012; Lang et al. 2004; Siebner et al. 2004). There seems to be a corresponding mechanism when using functional connectivity as an outcome measure. However, it is unclear if functional connectivity as a pure measure of synchronized BOLD-activation is sufficient to characterize stimulation effects. Additional outcome variables such as neurotransmitter release in connected areas, and both short and more long term functional parameters will be important to observe in methodological and clinical research.

Some authors have linked lDLPFC stimulation to visual hallucinations (Blanke et al. 2000), while others showed a decrease in auditory verbal hallucinations after frontal-temporal tDCS treatment (Rashidi et al. 2021). Interestingly, in a study on psychosis that did not use brain stimulation, patients showed decreased connectivity between the bilateral Heschl's gyri and the dorsal anterior cingulate cortex, but increased connectivity between the planum temporale and the right dorsolateral prefrontal cortex (Yoon et al. 2015). In our study both Heschl's gyrus and planum temporale showed similar pattern of functional connectivity to the DLPFC and the striatum, and differed significantly between the anodal and the cathodal group both after tDCS, as well as after TMS. The principle of modulating fronto-temporo-parietal connectivity with preconditioning, that was proven in this study, might be relevant for further research into hallucination and psychosis treatment.

Some authors argue that the mere peripheral stimulation administered by the different tDCS protocols can contribute to observed results, especially since the precise neuronal mechanisms of tDCS remain unclear (Asamoah et al. 2019). Some even state that the commonly used dose of 1mV is too small to induce actual physiological changes in the brain (Vöröslakos et al. 2018). However, this was argued for the motor system and authors did not study functional network connectivity.

The main limitations of this study is the relatively low number of participants per group and the resulting reduced statistical power due to the complex experimental design. Given the high level of variation in BOLD activity and the very high number of comparisons in the statistical analysis increasing the number of observations would give clearer results. Additionally, we acknowledge that the choice of stimulation site as well as stimulation protocols is rather arbitrary due to lack of previous studies on this particular area. Although we used a TMS protocol that has previously been shown to increase frontostriatal functional connectivity (Alkhasli et al. 2019; Strafella et al. 2001), it is not clear whether the tDCS and TMS protocols used in the present study are able to induce a strong short-term potentiation effect in the prefrontal cortex and its connected areas. We did include only healthy and young participants and were not aiming for long-term effects. However, the potential for a therapeutic use preconditioning is very evident, as it was shown that cortical-subcortical communication can be modulated by non-invasive brain-stimulation. It remains an important question whether preconditioning can help induce long-term changes in connectivity and activation levels, that are needed in therapeutic settings. Different

stimulation protocols, sites and timelines, as well as potential clinical outcome variables for different patient groups, such as patients with mood disorders or neurodegenerative disorders should be studied systematically.

Conclusion

This study is the first combining tDCS and rTMS to demonstrate, as a proof of principle, a preconditioning and modulatory effect of the dorsolateral prefrontal cortex and its connectivity to the anterior cingulate, paracingulate, insular cortex, operculum, Heschl's gyrus, as well as the striatum. Application of excitatory iTBS to a tDCS-inhibited prefrontal cortex yielded a stronger activity in terms of functional connectivity than excitatory iTBS to a tDCS-enhanced prefrontal cortex. Our results demonstrate a complex whole brain impact of brain stimulation on functional connectivity, as well as the importance of the pre-existing state of neural networks on stimulation outcomes. There needs to be more research into different stimulation protocols and the possibility to modulate activity of connected sub-cortical areas, as well as a potential therapeutic use.

Abbreviations

tDCS Transcranial direct current stimulation

rsfMRI Resting state functional magnetic resonance imaging

TMS Transcranial magnetic stimulation

iTBS Intermittent theta burst stimulation

ANOVA Analysis of variance

rMT Resting motor threshold

lDLPFC Left dorsolateral prefrontal cortex

BOLD Blood oxygenation level dependent

Declarations

Author Contributions

Theoretical considerations, experimental design and experimental plan were prepared by Katrin Sakreida, Ferdinand Binkofski and Felix Mottaghy. The experimental setup and data collection was conducted by Katrin Sakreida and Isabel Alkhasli. Data management and processing, statistical analysis and manuscript preparation was carried out by Isabel Alkhasli.

All authors contributed to the final version of the manuscript and approved it.

Funding

This work was supported by the START program of the Faculty of Medicine at RWTH Aachen University (grant number 12/16).

Conflict of Interest

The authors declare that the research was conducted in the absence of any non-financial or financial relationships that could be construed as a potential conflict of interest.

Acknowledgement

The authors thank Meike Schulte for her valuable help during data collection and LOCALITE Biomedical Visualization Systems GmbH (Sankt Augustin, Germany) for technical support.

Data Availability

The datasets generated during and/or analysed during the current study are available from the corresponding author on reasonable request.

Compliance with Ethical Standards

Our study was approved by the ethical committee of the RWTH university hospital (EK 357/15) and all procedures involving human participants were in accordance with the ethical standards of the institutional and/or national research committee and with the 1964 Helsinki declaration and its later amendments or comparable ethical standards. Informed consent was obtained from all individual participants included in the study.

References

1. Alexander GE, DeLong MR, Strick PL (1986) Parallel organization of functionally segregated circuits linking basal ganglia and cortex. Annual review of neuroscience 9:357–381. https://doi.org/10.1146/annurev.ne.09.030186.002041
2. Alkhasli I, Sakreida K, Mottaghy FM, Binkofski F (2019) Modulation of frontostriatal functional connectivity using transcranial magnetic stimulation. Frontiers in human neuroscience 13:190. https://doi.org/10.3389/fnhum.2019.00190
3. Arnsten AFT (2009) Stress signalling pathways that impair prefrontal cortex structure and function. Nature reviews neuroscience 10:410–422. https://doi.org/10.1038/nrn2648
4. Asamoah B, Khatoun A, Mc Laughlin M (2019) tACS motor system effects can be caused by transcutaneous stimulation of peripheral nerves. Nat Commun 10:1–16
5. Asanuma H, Keller A (1991) Neurobiological basis of motor learning and memory. Concepts neurosci 2:1–30

6. Bear MF, Malenka RC (1994) Synaptic plasticity: LTP and LTD. Current opinion in neurobiology 4:389–399. https://doi.org/10.1016/0959-4388(94)90101-5
7. Benjamini Y, Hochberg Y (1995) Controlling the false discovery rate: a practical and powerful approach to multiple testing. Journal of the royal statistical society: series B (Methodological) 57:289–300. https://doi.org/10.1111/j.2517-6161.1995.tb02031.x
8. Bestmann S, Baudewig J, Siebner HR, Rothwell JC, Frahm J (2004) Functional MRI of the immediate impact of transcranial magnetic stimulation on cortical and subcortical motor circuits. European journal of neuroscience 19:1950–1962. https://doi.org/10.1111/j.1460-9568.2004.03277.x
9. Bradley MM, Lang PJ (1994) Measuring emotion: the self-assessment manikin and the semantic differential. Journal of behavior therapy and experimental psychiatry 25:49–59. https://doi.org/10.1016/0005-7916(94)90063-9
10. Carlsson M, Carlsson A (1990) Interactions between glutamatergic and monoaminergic systems within the basal ganglia-implications for schizophrenia and Parkinson's disease. Trends in neurosciences 13:272–276. https://doi.org/10.1016/0166-2236(90)90108-m
11. Carnevali L, Pattini E, Sgoifo A, Ottaviani C (2020) Effects of prefrontal transcranial direct current stimulation on autonomic and neuroendocrine responses to psychosocial stress in healthy humans. Stress 23:26–36. https://doi.org/10.1080/10253890.2019.1625884
12. Carvalho S, Boggio PS, Gonçalves ÓF, Vigário AR, Faria M, Silva S, do Rego GG, Fregni F, Leite J (2015) Transcranial direct current stimulation based metaplasticity protocols in working memory. Brain stimulation 8:289–294
13. Cosentino G, Fierro B, Paladino P, Talamanca S, Vigneri S, Palermo A, Giglia G, Brighina F (2012) Transcranial direct current stimulation preconditioning modulates the effect of high-frequency repetitive transcranial magnetic stimulation in the human motor cortex. European journal of neuroscience 35:119–124. https://doi.org/10.1111/j.1460-9568.2011.07939.x
14. Dedoncker J, Brunoni AR, Baeken C, Vanderhasselt M-A (2016) A systematic review and meta-analysis of the effects of transcranial direct current stimulation (tDCS) over the dorsolateral prefrontal cortex in healthy and neuropsychiatric samples: influence of stimulation parameters. Brain stimulation 9:501–517. https://doi.org/10.1016/j.brs.2016.04.006
15. Eickhoff SB, Amunts K, Mohlberg H, Zilles K (2006) The human parietal operculum. II. Stereotaxic maps and correlation with functional imaging results. Cerebral cortex 16:268–279. https://doi.org/10.1093/cercor/bhi106
16. Fox MD, Halko MA, Eldaief MC, Pascual-Leone A (2012) Measuring and manipulating brain connectivity with resting state functional connectivity magnetic resonance imaging (fcMRI) and transcranial magnetic stimulation (TMS). Neuroimage 62:2232–2243. https://doi.org/10.1016/j.neuroimage.2012.03.035
17. Fregni F, Pascual-Leone A (2007) Technology insight: noninvasive brain stimulation in neurology—perspectives on the therapeutic potential of rTMS and tDCS. Nature clinical practice neurology 3:383–393. https://doi.org/10.1038/ncpneuro0530

18. Fricke K, Seeber AA, Thirugnanasambandam N, Paulus W, Nitsche MA, Rothwell JC (2011) Time course of the induction of homeostatic plasticity generated by repeated transcranial direct current stimulation of the human motor cortex. Journal of neurophysiology 105:1141–1149. https://doi.org/10.1152/jn.00608.2009
19. Grüner U, Eggers C, Ameli M, Sarfeld A-S, Fink GR, Nowak DA (2010) 1 Hz rTMS preconditioned by tDCS over the primary motor cortex in Parkinson's disease: effects on bradykinesia of arm and hand. Journal of neural transmission 117:207–216. https://doi.org/10.1007/s00702-009-0356-0
20. Guse B, Falkai P, Wobrock T (2010) Cognitive effects of high-frequency repetitive transcranial magnetic stimulation: a systematic review. Journal of neural transmission 117:105–122. https://doi.org/10.1007/s00702-009-0333-7
21. Hess G, Donoghue JP (1996) Long-term depression of horizontal connections in rat motor cortex. European journal of neuroscience 8:658–665. https://doi.org/10.1111/j.1460-9568.1996.tb01251.x
22. Huang Y-Z, Edwards MJ, Rounis E, Bhatia KP, Rothwell JC (2005) Theta burst stimulation of the human motor cortex. Neuron 45:201–206. https://doi.org/10.1016/j.neuron.2004.12.033
23. Iriki A, Pavlides C, Keller A, Asanuma H (1989) Long-term potentiation in the motor cortex. Science 245:1385–1387. https://doi.org/10.1126/science.2551038
24. Kähkönen S, Komssi S, Wilenius J, Ilmoniemi RJ (2005) Prefrontal TMS produces smaller EEG responses than motor-cortex TMS: implications for rTMS treatment in depression. Psychopharmacology 181:16–20. https://doi.org/10.1007/s00213-005-2197-3
25. Kanno M, Matsumoto M, Togashi H, Yoshioka M, Mano Y (2004) Effects of acute repetitive transcranial magnetic stimulation on dopamine release in the rat dorsolateral striatum. Journal of the neurological sciences 217:73–81. https://doi.org/10.1016/j.jns.2003.08.013
26. Karreman M, Moghaddam B (1996) The prefrontal cortex regulates the basal release of dopamine in the limbic striatum: an effect mediated by ventral tegmental area. Journal of neurochemistry 66:589–598
27. Keck ME, Welt T, Müller MB, Erhardt A, Ohl F, Toschi N, Holsboer F, Sillaber I (2002) Repetitive transcranial magnetic stimulation increases the release of dopamine in the mesolimbic and mesostriatal system. Neuropharmacology 43:101–109. https://doi.org/10.1016/S0028-3908(02)00069-2
28. Keeser D, Meindl T, Bor J, Palm U, Pogarell O, Mulert C, Brunelin J, Möller H-J, Reiser M, Padberg F (2011) Prefrontal transcranial direct current stimulation changes connectivity of resting-state networks during fMRI. Journal of neuroscience 31:15284–15293. https://doi.org/10.1523/JNEUROSCI.0542-11.2011
29. Lang N, Siebner HR, Ernst D, Nitsche MA, Paulus W, Lemon RN, Rothwell JC (2004) Preconditioning with transcranial direct current stimulation sensitizes the motor cortex to rapid-rate transcranial magnetic stimulation and controls the direction of after-effects. Biological psychiatry 56:634–639. https://doi.org/10.1016/j.biopsych.2004.07.017

30. Murase S, Grenhoff J, Chouvet G, Gonon FG, Svensson TH (1993) Prefrontal cortex regulates burst firing and transmitter release in rat mesolimbic dopamine neurons studied in vivo. Neuroscience letters 157:53–56. https://doi.org/10.1016/0304-3940(93)90641-W
31. Nahas Z, Lomarev M, Roberts DR, Shastri A, Lorberbaum JP, Teneback C, McConnell K, Vincent DJ, Li X, George MS (2001) Unilateral left prefrontal transcranial magnetic stimulation (TMS) produces intensity-dependent bilateral effects as measured by interleaved BOLD fMRI. Biological psychiatry 50:712–720. https://doi.org/10.1016/S0006-3223(01)01199-4
32. OIdfleld RC (1971) The assessment and analysis of handedness: the Edinburgh inventory. Neuropsyehologia
33. Paus T, Castro-Alamancos MA, Petrides M (2001) Cortico-cortical connectivity of the human mid-dorsolateral frontal cortex and its modulation by repetitive transcranial magnetic stimulation. European journal of neuroscience 14:1405–1411. https://doi.org/10.1046/j.0953-816x.2001.01757.x
34. Petrides M, Pandya DN (1999) Dorsolateral prefrontal cortex: comparative cytoarchitectonic analysis in the human and the macaque brain and corticocortical connection patterns. European journal of neuroscience 11:1011–1036. https://doi.org/10.1046/j.1460-9568.1999.00518.x
35. Rioult-Pedotti M-S, Friedman D, Donoghue JP (2000) Learning-induced LTP in neocortex. Science 290:533–536. https://doi.org/10.1126/science.290.5491.533
36. Rossi S, Hallett M, Rossini PM, Pascual-Leone A, Safety of TMS Consensus Group (2009) Safety, ethical considerations, and application guidelines for the use of transcranial magnetic stimulation in clinical practice and research. Clinical neurophysiology 120:2008–2039. https://doi.org/10.1016/j.clinph.2009.08.016
37. Rossini PM, Burke D, Chen R, Cohen LG, Daskalakis Z, Di Iorio R, Di Lazzaro V, Ferreri F, Fitzgerald PB, George MS (2015) Non-invasive electrical and magnetic stimulation of the brain, spinal cord, roots and peripheral nerves: basic principles and procedures for routine clinical and research application. An updated report from an IFCN Committee. Clinical neurophysiology 126:1071–1107
38. Rusjan PM, Barr MS, Farzan F, Arenovich T, Maller JJ, Fitzgerald PB, Daskalakis ZJ (2010) Optimal transcranial magnetic stimulation coil placement for targeting the dorsolateral prefrontal cortex using novel magnetic resonance image-guided neuronavigation. Human brain mapping 31:1643–1652. https://doi.org/10.1002/hbm.20964
39. Sawamoto N, Honda M, Okada T, Hanakawa T, Kanda M, Fukuyama H, Konishi J, Shibasaki H (2000) Expectation of pain enhances responses to nonpainful somatosensory stimulation in the anterior cingulate cortex and parietal operculum/posterior insula: an event-related functional magnetic resonance imaging study. Journal of neuroscience 20:7438–7445
40. Shafi MM, Westover MB, Fox MD, Pascual-Leone A (2012) Exploration and modulation of brain network interactions with noninvasive brain stimulation in combination with neuroimaging. European journal of neuroscience 35:805–825. https://doi.org/10.1111/j.1460-9568.2012.08035.x
41. Siebner HR, Lang N, Rizzo V, Nitsche MA, Paulus W, Lemon RN, Rothwell JC (2004) Preconditioning of low-frequency repetitive transcranial magnetic stimulation with transcranial direct current

stimulation: evidence for homeostatic plasticity in the human motor cortex. Journal of neuroscience 24:3379–3385. https://doi.org/10.1523/JNEUROSCI.5316-03.2004

42. Siebner HR, Willoch F, Peller M, Auer C, Boecker H, Conrad B, Bartenstein P (1998) Imaging brain activation induced by long trains of repetitive transcranial magnetic stimulation. Neuroreport 9:943–948. https://doi.org/10.1097/00001756-199803300-00033
43. Sparing R, Mottaghy FM (2008) Noninvasive brain stimulation with transcranial magnetic or direct current stimulation (TMS/tDCS)—from insights into human memory to therapy of its dysfunction. Methods 44:329–337. https://doi.org/10.1016/j.ymeth.2007.02.001
44. Strafella AP, Paus T, Barrett J, Dagher A (2001) Repetitive transcranial magnetic stimulation of the human prefrontal cortex induces dopamine release in the caudate nucleus. Journal of neuroscience 21:RC157-RC157. https://doi.org/10.1523/JNEUROSCI.21-15-j0003.2001
45. Strafella AP, Paus T, Fraraccio M, Dagher A (2003) Striatal dopamine release induced by repetitive transcranial magnetic stimulation of the human motor cortex. Brain 126:2609–2615. https://doi.org/10.1093/brain/awg268
46. Strafella AP, Ko JH, Grant J, Fraraccio M, Monchi O (2005) Corticostriatal functional interactions in Parkinson's disease: a rTMS/[11C] raclopride PET study. European journal of neuroscience 22:2946–2952. https://doi.org/10.1111/j.1460-9568.2005.04476.x
47. Tekin S, Cummings JL (2002) Frontal–subcortical neuronal circuits and clinical neuropsychiatry: an update. Journal of psychosomatic research 53:647–654. https://doi.org/10.1016/S0022-3999(02)00428-2
48. Tik M, Hoffmann A, Sladky R, Tomova L, Hummer A, Lara LN de, Bukowski H, Pripfl J, Biswal B, Lamm C (2017) Towards understanding rTMS mechanism of action: stimulation of the DLPFC causes network-specific increase in functional connectivity. Neuroimage 162:289–296. https://doi.org/10.1016/j.neuroimage.2017.09.022
49. Tremblay S, Lepage J-F, Latulipe-Loiselle A, Fregni F, Pascual-Leone A, Théoret H (2014) The uncertain outcome of prefrontal tDCS. Brain stimulation 7:773–783. https://doi.org/10.1016/j.brs.2014.10.003
50. Vöröslakos M, Takeuchi Y, Brinyiczki K, Zombori T, Oliva A, Fernández-Ruiz A, Kozák G, Kincses ZT, Iványi B, Buzsáki G, Berényi A (2018) Direct effects of transcranial electric stimulation on brain circuits in rats and humans. Nat Commun 9:483. https://doi.org/10.1038/s41467-018-02928-3
51. Whitfield-Gabrieli S, Nieto-Castanon A (2012) Conn: a functional connectivity toolbox for correlated and anticorrelated brain networks. Brain connectivity 2:125–141. https://doi.org/10.1089/brain.2012.0073
52. Wunderlich AP, Klug R, Stuber G, Landwehrmeyer B, Weber F, Freund W (2011) Caudate nucleus and insular activation during a pain suppression paradigm comparing thermal and electrical stimulation. The open neuroimaging journal 5:1. https://doi.org/10.2174/1874440001105010001

Tables

Table 1. Seed-to-Voxel-Results: Interaction-Contrast Results						
Cluster peak (x, y, z)	**Voxels**	**Size *p* (FDR)**	**Size *p* (unc.)**	**Anatomical classification**		
				Voxels	**Region**	**% of Region**
4, 30, 14	1638	> .000	> .000	399	anterior cingulate gyrus	15
(fronto-cingulate cluster)				144	l. frontal pole	2
				128	r. paracingulate gyrus	9
				121	l. paracingulate gyrus	9
				75	r. superior frontal gyrus	3
				23	l. caudate	4
				10	r. frontal pole	<1
				8	l. superior frontal gyrus	<1
				8	r. caudate	2
-44, -26, 14	479	.015	> .000	215	l. central opercular cortex	22
(left temporo-parietal cluster)				100	l. Heschl's gyrus	32
				69	l. insular cortex	5
				66	l. parietal operculum	12
				12	l. planum temporale	2
				1	l. planum polare	<1
42, -16, 8	583	.006	> .000	105	r. insular cortex	8
(right temporo-parietal cluster)				103	r. planum temporale	23
				101	r. central opercular cortex	12
				90	r. parietal operculum	17
				83	r. Heschl's Gyrus	29
				6	r. postcentral gyrus	<1
				1	r. anterior supramar. gyrus	<1

Results of seed-to-voxel analysis. A 2 x 2 contrast (Anodal vs cathodal and post tDCS vs post TMS) was calculated between the mean signal of the spherical stimulation site seed and each individual voxel of the rest of the whole brain masks. The alpha-level was kept at 5% (uncorrected on the voxel level and FDR-corrected on the cluster level for multiple comparison). Three big clusters were significant. Number of voxels as well as an anatomical classification as done automated by the Matlab/SPM toolbox CONN based on the Harvard-Oxford and AAL atlas are listed. Numbers in the last column indicate the percentage of significant voxels of the atlas region listed. *p = p-value, l. = left, r. = right*

Table 2. Results of Planned Post-Hoc T-Tests of ROI to ROI Data				
Time points	**Groups**	**Statistics**	**p-FDR**	**Sig. connections**
Baseline x post tDCS x post TMS	**Sham x Anodal x Cathodal**	F(4,52)	> .0500	none
Baseline x post tDCS x post TMS	**Sham**	F(2,8)	> .0500	none
Post tDCS	**Anodal > Cathodal**	*F*(2,17) = 10.13 *T*(18) = 5.21 *T*(18) = 3.45 *T*(18) = 2.66 *T*(18) = 2.16 *F*(2,17) = 6.67 *T*(18) = 4.35	.0038 .0002 .0038 .0632 .0887 .0109 .0008	**Cluster 1** lDLPFC x l. temporo-parietal cluster lDLPFC x r. temporo-parietal cluster Striatum x r. temporo-parietal cluster Fronto-cingulate x l. temporo-parietal cluster **Cluster 2** lDLPFC x Fronto-cingulate cluster
	Anodal > Sham	*F*(2,17) = 5.80 *T*(18) = 3.62	.0361 .0079	**Cluster 1** lDLPFC x Fronto-cingulate cluster
	Cathodal > Sham	*T*(18)	> .0500	None
Post TMS	**Anodal > Cathodal**	*F*(2,17) = 7.83 *T*(18) = -4.07 *F*(2,17) = 5.96	.0117 .0029 .0164 .0255 .0433	**Cluster 1** lDLPFC x Fronto-cingulate cluster **Cluster 2** lDLPFC x r. temporo-parietal cluster lDLPFC x l. temporo-parietal cluster

	T(18) = -2.77	.0863	Striatum x l. temporo-parietal cluster
	T(18) = -2.32		
	T(18) = 2.52		
Anodal > Sham	*T*(18)	> .0500	none
Cathodal > Sham	*F*(2,17) = 7.40	.0146	**Cluster 1**
		.0094	lDLPFC x Fronto-cingulate cluster
	T(18) = 3.54	.1484	lDLPFC x striatum
	T(18) = 2.25	.0407	**Cluster 2**
	F(1,18) = 5.78	.1087	L. x r. temporo-parietal cluster
	T(18) = 2.40		

Results of ROI-to-ROI analysis. ANOVAs and post-hoc t-tests where calculated to test functional network connectivity between the mean signal of the five ROIs. The alpha-level was kept at 5% (FDR-corrected on the cluster level and uncorrected on the connection level). Additional connections, that were not revealed by the seed-to-voxel analysis are marked by an underscore. Those were a striatal-right temporo-parietal and fronto-cingulate-left temporo-parietal difference between the anodal and cathodal groups in the post tDCS and striatal-left temporo-parietal differences between the anodal and cathodal groups in the post TMS measurements as well as a left-right temporo-parietal difference between the cathodal and sham group post TMS. p = p-value. L/l = left, r = right.

Figures

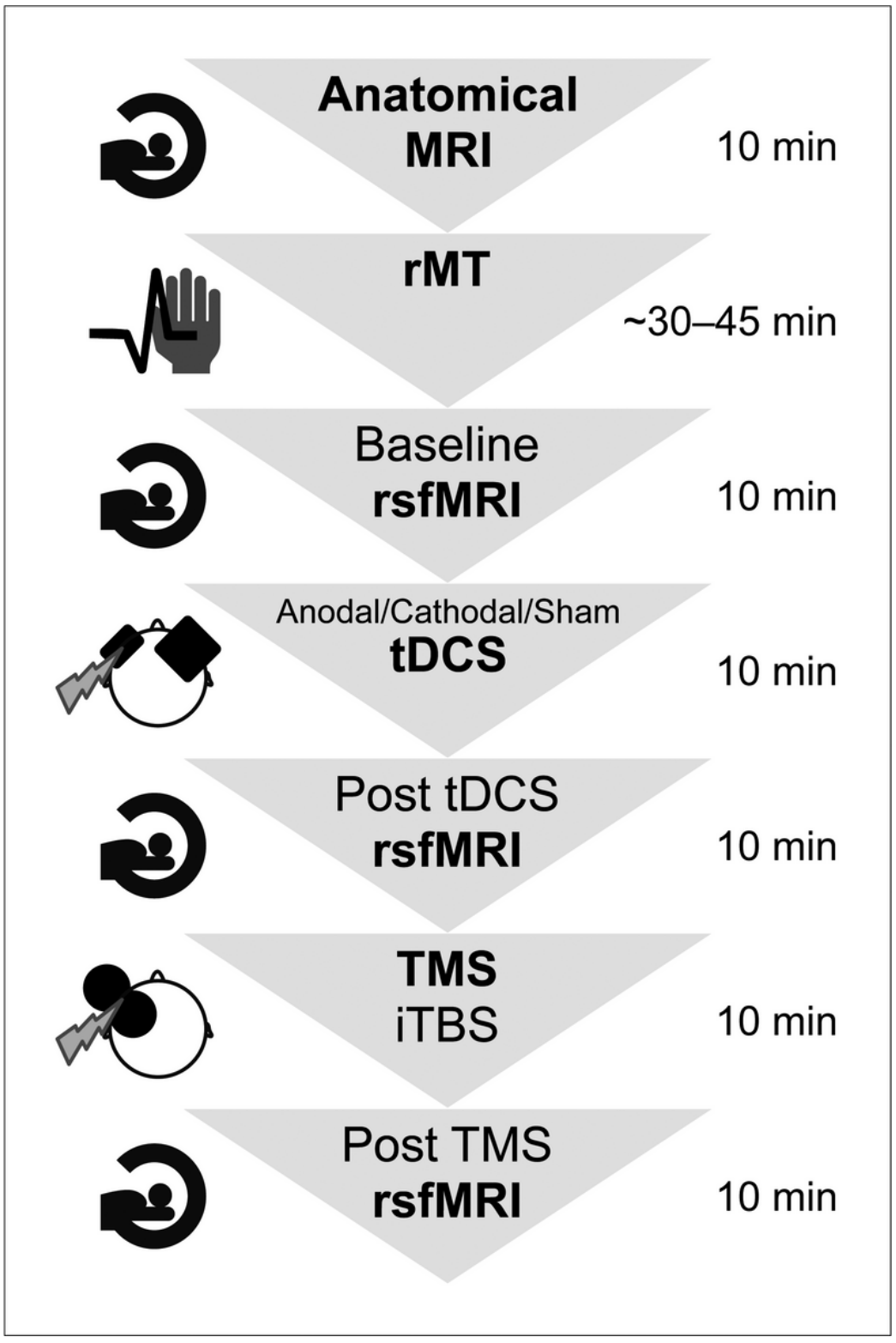

Figure 1

Summary of the Experimental Design and Durations. First, the participants entered the MRI scanner for 10 min to create anatomical images. Afterwards their individual resting motor threshold was determined, which took approximately 45 min. The experiment comprised two brain stimulation sessions as well as three functional resting state functional MRI scans lasting approximately 10 min each. The whole experimental procedure took in total approximately 2 hours per participant. *rsfMRI = resting state*

functional magnetic resonance imaging, rMT = resting motor threshold, tDCS = transcranial direct current stimulation, TMS = transcranial magnetic stimulation, iTBS = intermittent theta burst stimulation.

(Created using Adobe Illustrator 2021, single-column width 84 mm, grayscale)

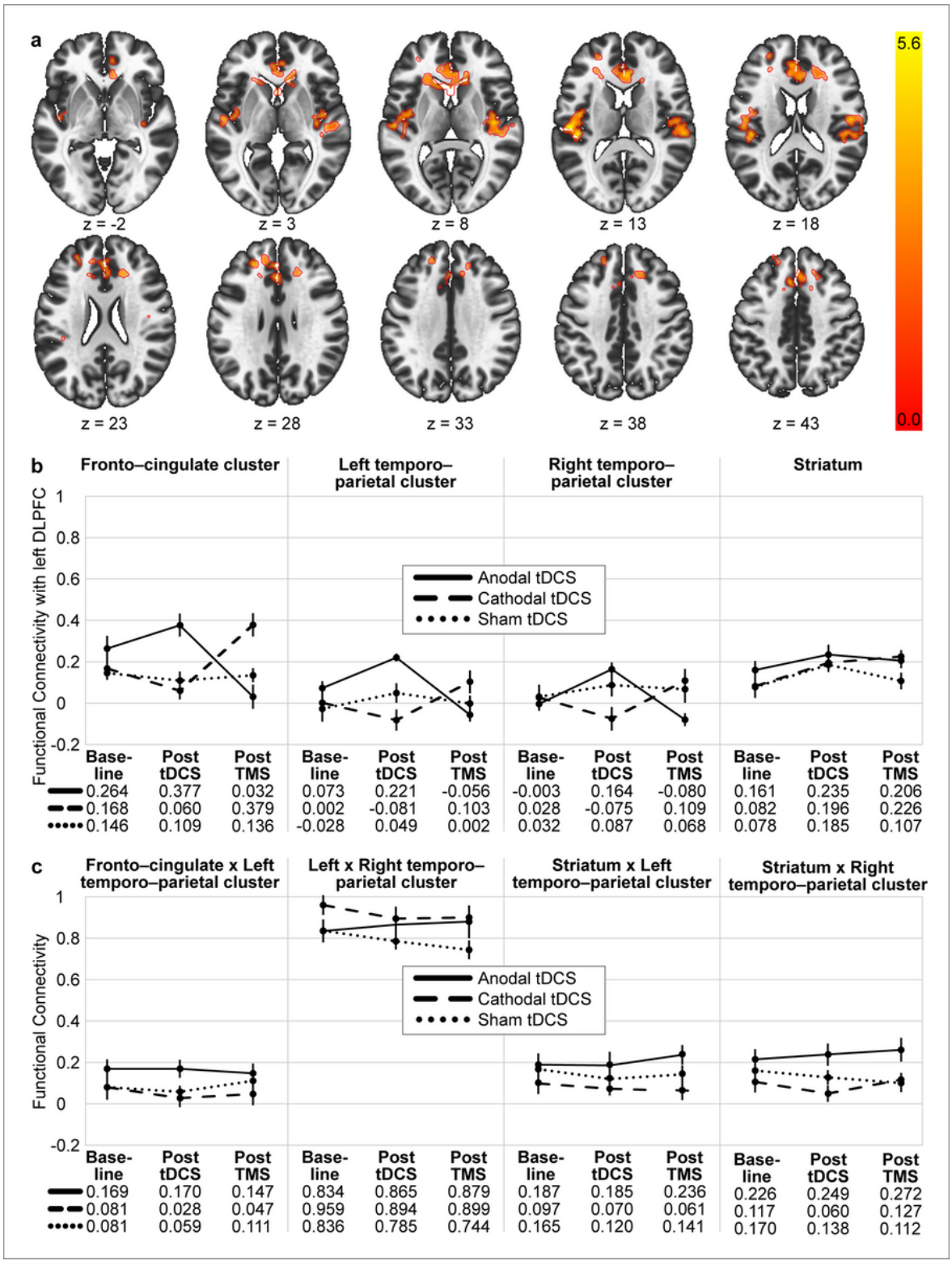

Figure 2

Visualisation of the seed-to-voxel and ROI-to-ROI analysis results. a) Significant voxel and cluster location for the seed-to-voxel analysis with the 2 × 2 contrast: anodal > cathodal and post tDCS > post TMS. The coloured scale indicates T-values of significant voxels. b) Each diagram represents the mean functional connectivity in the three groups (anodal, cathodal and sham tDCS) and three time points (baseline, post tDCS and post TMS) and between the stimulation site and three significant clusters and the striatum, respectively. c) Diagrams of mean functional connectivity values for each group and time point and four additional significant ROI-to-ROI connections. Error bars represent standard errors. *Anodal tDCS = solid line, cathodal tDCS= dashed line, sham tDCS= dotted line.*

(Created using CONN toolbox, Matlab, and Adobe Illustrator 2021, double-column width 176 mm, coloured)